The minimum-time trajectories for an omni-directional vehicle

Devin J. Balkcom[1], Paritosh A. Kavathekar[1], and Matthew T. Mason[2]

[1] Dartmouth Computer Science Department
{devin, paritosh}@cs.dartmouth.edu
[2] Carnegie Mellon Robotics Institute
matt.mason@cs.cmu.edu

Abstract: One common mobile robot design consists of three 'omniwheels' arranged at the vertices of an equilateral triangle, with wheel axles aligned with the rays from the center of the triangle to each wheel. Omniwheels, like standard wheels, are driven by the motors in a direction perpendicular to the wheel axle, but unlike standard wheels, can slip in a direction parallel to the axle. Unlike a steered car, a vehicle with this design can move in any direction without needing to rotate first, and can spin as it does so. We show that if there are independent bounds on the speeds of the wheels, the fastest trajectories for this vehicle contain only spins in place, circular arcs, and straight lines parallel to the wheel axles. We classify optimal trajectories by the order and type of the segments; there are four such classes, and there are no more than 18 control switches in any optimal trajectory.

1 Introduction

This paper presents the time-optimal trajectories for a simple model of the common mobile-robot design shown in figure 1(b). The three wheels are "omni-wheels"; the wheels not only rotate forwards and backwards when driven by the motors, but can also slip sideways freely. Such a robot can drive in any direction instantaneously.

The only other ground vehicles for which the fastest trajectories are known explicitly are steered cars and differential-drives. Although our results are specific to the particular vehicle studied, we hope that expanding the set of vehicles for which the optimal trajectories are known will eventually lead to a more unified understanding of the relationship between robot mechanism design and the use of resources.

We show that the time-optimal trajectories consist of spins in place, circular arcs, and straight lines parallel to the wheel axles. We label each segment type by a letter: P, C, S, respectively. There are specific sequences of segments that may be optimal; we call the four possible classes of trajectories *spin*, *roll*, *shuffle*, and *tangent*. Figures 3(a), 4(a), 4(b), and 4(c) show an example of each type.

1. *Spin* trajectories consist of a spin in place through an angle no greater than π, and are described by the single-letter control sequence P.

2. *Roll* trajectories consist of a sequence of up to five circular arcs of equal radius separated by spins in place, and are described by the control sequence CPCPC. The centers of the arcs all fall on a straight line. With the possible exception of the first and last segments, the arcs all encompass the same angle, as do the spins, and the sum of the angular displacement of a complete arc and a complete spin is $120°$.
3. *Shuffle* trajectories are composed of sequences of three circular arcs followed by a spin, CCCP, and contain no more than seven control switches. A complete period of a *shuffle* moves the vehicle 'sideways' in a direction parallel to a line connecting two wheels.
4. *Tangent* trajectories consist of a sequence of arcs of circles and spins in place separated by arbitrarily long translations in a direction parallel to the line containing the center of the robot and one of its wheels. All straight segments are colinear. The control sequence is CSCSCP, and trajectories contain no more than 18 switches. Intuitively, the robot 'lines up' in its fastest direction of translation, translates, and then follows arcs of circles to arrive at its final position and orientation.

Why study optimal trajectories? Knowledge of the shortest or fastest paths between any two configurations of a particular robot is fundamental. Robots expend resources to achieve tasks. Possibly the simplest resource is time; the amount of time that must be expended to move the robot between configurations is a basic property of the mechanism, and a fundamental metric on the configuration space.

Knowledge of the time optimal trajectories is also useful. Mechanisms should be designed so that common tasks can be achieved efficiently. If the designer must choose between two wheels and three, what is the cost of each choice? Furthermore, the time-optimal metric is independent of software-design decisions, and therefore provides a benchmark to compare planners or controllers. Finally, the metric derived from the optimal trajectories may be used as a heuristic to guide sampling in complete planning systems that permit obstacles or a more complex dynamic model of the mechanism.

We do not argue that controllers should be designed to drive robots to follow the 'optimal' trajectories we derive, or that planners must use the optimal trajectories as building blocks. In fact, resources other than time may also be important, including

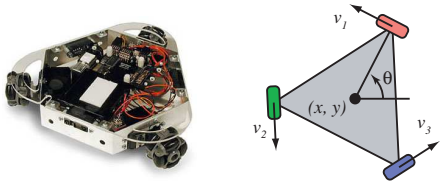

(a) Photograph. (b) Notation.

Fig. 1: The Palm-Pilot Robot Kit, an example of an omni-directional vehicle. Photograph used by permission of Acroname, Inc., `www.acroname.com`.

energy consumption, safety, simplicity of programming, sensing opportunities, and accuracy. Tradeoffs must be made, but understanding the relative payoffs of each design requires an understanding of the fundamental behavior of the mechanism. The knowledge that great circles are geodesics on the sphere does not require that airplanes must strictly follow great circles, but may nonetheless influence the choice of flight paths.

1.1 Related work

Most of the work on time-optimal control for vehicles has focused on bounded-velocity models of steered cars. Dubins [6] determined the shortest paths between two configurations of a car that can only move forwards at constant speed, with bounded steering angle. Reeds and Shepp [9] found the shortest paths for a steered car that can move backwards as well as forwards. Sussmann and Tang [14] further refined these results, reducing the number of families of trajectories thought to be optimal by two, and Souères and Boissonnat [12], and Souères and Laumond [13] discovered the mapping from pairs of configurations to optimal trajectories for the Reeds and Shepp car. Desaulniers [5] showed that in the presence of obstacles shortest paths may not exist between certain configurations of steered cars. Furthermore, in addition to the straight lines and circular arcs of minimum radius discovered by Dubins, the shortest paths may also contain segments that follow the boundaries of obstacles. Vendittelli *et al.* [15] used geometric techniques to develop an algorithm to obtain the shortest non-holonomic distance from a robot to any point on an obstacle.

Recently, the optimal trajectories have been found for vehicles that are not steered cars, and metrics other than time. The time-optimal controls for bounded-velocity differential-drives were discovered by Balkcom and Mason [1]. Chitsaz *et al.* [2] determined the trajectories for a differential-drive that minimize the sum of the rotation of the two wheels. The optimal paths have also been explored for some examples of vehicles without wheels. Coombs and Lewis [4] consider a simplified model of a hovercraft, and Chyba and Haberkorn [3] consider underwater vehicles. We know of no previous attempts to obtain closed-form solution for the optimal trajectories for any omni-directional vehicle.

Bounded-velocity models capture the kinematics of a vehicle, but not the dynamics. The results of this paper strongly depend on the analytical solution of differential equations describing the optimal trajectories. Analysis of dynamic models, for which analytical solutions are not typically available, is a very difficult problem. Results include numerical techniques and geometric characterization rather than complete closed-form solutions; see papers by Reister and Pin [10], Renaud and Fourquet [11], and Kalmár-Nagy *et al.* [7].

2 Model, assumptions, notation

Let the state of the robot be $q = (x, y, \theta)$, the location of the center of the robot, and the angle that the line from the center to the first wheel makes with the horizontal, as shown in figure 1(b). Without loss of generality, we assume that the distance from

the center of the robot to the wheels is one. We further assume that each of the three wheel-speed controls v_1, v_2, and v_3 is in the interval $[-1, 1]$. We define the control region

$$U = [-1, 1] \times [-1, 1] \times [-1, 1], \tag{1}$$

and consider the class of *admissible controls* to be the measurable functions $u(t)$ mapping the time interval $[0, T]$ to U: $u(t) = (v_1(t), v_2(t), v_3(t))^T$.

To simplify notation, we define $c_i = \cos\theta_i$, and $s_i = \sin\theta_i$, where $\theta_i = \theta + (i - 1)120°$, the angle of the ith wheel measured from the horizontal. Define the matrix S to be the Jacobian that transforms between configuration-space velocities of the vehicle, and velocities of the wheels in the controlled direction:

$$S = \begin{bmatrix} -s_1 & c_1 & 1 \\ -s_2 & c_2 & 1 \\ -s_3 & c_3 & 1 \end{bmatrix}, \qquad S^{-1} = \tfrac{2}{3} \begin{bmatrix} -s_1 & -s_2 & -s_3 \\ c_1 & c_2 & c_3 \\ 1/2 & 1/2 & 1/2 \end{bmatrix}. \tag{2}$$

We define the state trajectory $q(t) = (x(t), y(t), \theta(t))$ for any initial state q_0 and admissible control $u(t)$ using Lebesgue integration, with the standard measure:

$$q(t) = q_0 + \int S^{-1} u \, . \tag{3}$$

It may be easily verified that the kinematic equations and bounds on the controls satisfy the conditions of theorem 6 of Sussmann and Tang [14]; an optimal trajectory exists between every pair of start and goal configurations.

3 Pontryagin's Maximum Principle

This section uses Pontryagin's Maximum Principle [8] to derive necessary conditions for time-optimal trajectories. The Maximum Principle states that if the trajectory $q(t)$ with corresponding control $u(t)$ is time-optimal then the following conditions must hold:

1. There exists a non-trivial (not identically zero) *adjoint function*: an absolutely continuous $\mathbf{R}^3$-valued function of time, $\lambda(t)$, defined by a differential equation, the *adjoint equation*, in the configuration and in time-derivatives of the configuration:
$$\dot{\lambda} = -\frac{\partial}{\partial q} \langle \lambda, \dot{q}(q, u) \rangle \quad \text{a.e.} \tag{4}$$
We call the inner product appearing in equation 4 the *Hamiltonian*:
$$H(\lambda, q, u) = \langle \lambda, \dot{q}(q, u) \rangle. \tag{5}$$
2. The control $u(t)$ minimizes the Hamiltonian:
$$H(\lambda(t), q(t), u(t)) = \min_{z \in U} H(\lambda(t), q(t), z) \quad \text{a.e.} \tag{6}$$
Equation 6 is called the *minimization equation*.
3. The Hamiltonian is constant and non-positive over the trajectory. We define λ_0 as the negative of the value of the Hamiltonian; λ_0 is constant and non-negative for any optimal trajectory.

3.1 Application of the Maximum Principle

We solve for the adjoint vector by direct integration: $\lambda_1 = 3k_1$, $\lambda_2 = 3k_2$, and $\lambda_3 = 3(k_1 y - k_2 x + k_3)$, where $3k_1$, $3k_2$, and $3k_3$ are constants of integration. (The constant factor of 3 will simplify the form of equations 9 below.)

We now substitute the adjoint function into the minimization equation to determine necessary conditions for time-optimal trajectories. To simplify notation, we define three functions,

$$\varphi_i(t) = \langle \lambda(t), f_i(q(t)) \rangle, \tag{7}$$

where f_i is the ith column of S^{-1}. Explicitly, if we define the function

$$\eta(x, y) = k_1 y - k_2 x + k_3, \tag{8}$$

then the functions are:

$$\varphi_i = 2(-k_1 s_i + k_2 c_i) + \eta(x, y) \tag{9}$$

We may now write the equation for the Hamiltonian in terms of these functions and the controls v_1, v_2, and v_3:

$$H = \varphi_1 v_1 + \varphi_2 v_2 + \varphi_3 v_3. \tag{10}$$

The minimization condition of the Maximum Principle (condition 2, above) applied to equation 10 implies that if the function φ_i is negative, then v_i should be chosen to take its maximum possible value, 1, in order to minimize H. If the function φ_i is positive, then v_i should be chosen to be -1. Since the controls switch whenever one of the functions φ_i changes sign, we refer to the functions φ_i as *switching functions*.

Theorem 1. *For any time-optimal trajectory of the omni-directional vehicle, there exist constants k_1, k_2, and k_3, with $k_1^2 + k_2^2 + k_3^2 \neq 0$, such that at almost every time t, the value of the control v_i is determined by the sign of the switching function φ_i:*

$$v_i = \begin{cases} 1 & \text{if } \varphi_i < 0 \\ -1 & \text{if } \varphi_i > 0, \end{cases} \tag{11}$$

where the switching functions φ_1, φ_2, and φ_3 are given by equations 8, 9. Furthermore, the quantity λ_0 defined by

$$\lambda_0 = -H(\varphi_1, \varphi_2, \varphi_3) = |\varphi_1| + |\varphi_2| + |\varphi_3| \tag{12}$$

is constant along the trajectory.

Proof: Application of the Maximum Principle. ■

The Maximum Principle does not directly give information about the optimal controls in the case that one or more of the switching functions φ_i is zero. Theorems 7 and 8 in section 4 specifically address this case. The Maximum Principle also does not give information about the constants of integration, as these depend on the initial and final configurations of the robot. In this paper, we give the structure of trajectories as a function of these constants, but do not describe how to determine the constants except in a few cases.

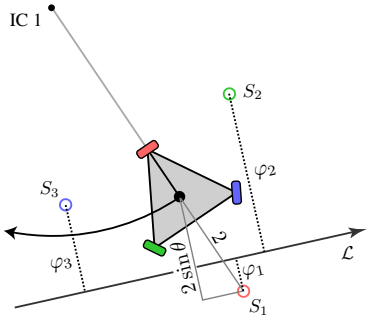

Fig. 2: Geometric interpretation of the switching functions. For the case shown, $\varphi_1 < 0$, $\varphi_2 > 0$, and $\varphi_3 > 0$, so the controls are $v_1 = 1$, $v_2 = -1$, and $v_3 = -1$.

3.2 Geometric interpretation of the switching functions

The switching functions are not independent, and have a geometric interpretation. Consider the function $\eta(x, y)$:

$$\eta(x, y) = k_1 y - k_2 x + k_3. \tag{13}$$

$\eta(x, y)$ gives the signed distance of the point (x, y) from a line in the plane whose location is determined by the constants k_1, k_2, and k_3, scaled by the factor $k_1^2 + k_2^2$. (If $k_1^2 + k_2^2 = 0$, we may consider the line to be 'at infinity'; the robot spins in place indefinitely. Since this control is identical to the *spin* trajectories described in section 5, we do not consider this case separately.) We will call this line the *switching line*. We also associate a direction with the switching line such that any point (x, y) is to the left of the switching line if $\eta(x, y) > 0$, and to the right of the switching line if $\eta(x, y) < 0$.

Theorem 2. *Define the points S_1, S_2, and S_3 rigidly attached to the vehicle, with distance 2 from the center of the vehicle, and making angles of $180°$, $300°$, and $60°$ with the ray from the center of the vehicle to wheel 1, respectively (refer to figure 2). For any time-optimal trajectory, there exist constants k_1, k_2, and k_3, and a line (the switching line)*

$$\mathcal{L} = \{(a, b) \in \mathbf{R}^2 : k_1 b - k_2 a + k_3 = 0\},$$

such that the controls of the vehicle v_1, v_2, and v_3 depend on the location of the points S_1, S_2, and S_3 relative to the line. Specifically, for $i \in \{1, 2, 3\}$,

$$v_i = \begin{cases} 1 & \text{if } S_i \text{ is to the right of the switching line,} \\ -1 & \text{if } S_i \text{ is to the left of the switching line.} \end{cases}$$

Proof: Let (x_{S_i}, y_{S_i}) be the coordinates of S_i. We compute the signed, scaled distance of the point S_i from the line $\mathcal{L}$, and observe from the definition of the switching functions that $\varphi_i(x, y, \theta) = \eta(x_{S_i}, y_{S_i})$. ■

We will call S_1, S_2, and S_3 the *switching points*. For any optimal trajectory, the location of the switching line is fixed by the choice of constants, and the controls at any point depend on the signs, but not on the magnitudes, of the switching functions. Figure 2 shows an example. Two of the switching points (S_2 and S_3) are to the left of the switching line, so the corresponding switching functions are positive, and wheels 2 and 3 spin at full speed in the negative direction. The remaining switching point (S_1) is to the right of the switching line, so wheel 1 spins at full speed in the positive direction. As a result of these controls, the robot will follow a clockwise circular arc. The center of the arc is a distance of four from the robot, and along the line containing the center of the robot and wheel 1.

In general, if all three switching functions have the same sign, the controls all take either their maximum or minimum value, and the robot spins in place. The center of rotation is the center of the robot; we call this point IC 0. If the switching functions are non-zero but do not all have the same sign, the vehicle rotates in a circular arc. The rotation center is a distance of four from the center of the robot, on the ray connect the center of the robot and the wheel corresponding to the 'minority' switching function. We call these rotation centers IC 1, IC 2, and IC 3.

The switching functions are invariant to translation of the vehicle parallel to the switching line (see figure 2), and scaling the switching functions by a positive constant does not affect the controls. Therefore, for any optimal trajectory, we may without loss of generality choose a coordinate frame with x-axis on the switching line, and an appropriate scaling, such that y gives the distance from the switching line, and θ gives the angle of the vehicle relative to the switching line. With this choice of coordinates, the switching functions become

$$\varphi_i = y - 2s_i \tag{14}$$

We will use these coordinates for the remainder of the paper.

4 Properties of extremals

We will say that any trajectory that satisfies the conditions of theorem 1 (or equivalently, theorem 2) is *extremal*. In this section, we will enumerate several properties of extremal trajectories. The primary result is that every extremal trajectory contains only a finite number of control switches with an upper bound determined by λ_0.

We say that an extremal trajectory is *generic* on some interval if none of the switching functions φ_i is zero at any point contained in the interval. We say that a trajectory is *singular* on some interval if exactly one of the switching functions is identically zero on that interval, and no other switching function is zero at any point on the interval. We say that an extremal trajectory is *doubly singular* on an interval if exactly two of the switching functions are zero on that interval, and the third switching function is never zero on the interval. We will call a trajectory *singular* if it contains any singular interval of non-zero width.

Detailed proofs of the following properties are omitted due to space limitations, but are available from the authors upon request. Most of the proofs are based on differential analysis of the switching functions.

Theorem 3. *At no point along an extremal trajectory does* $\varphi_1 = \varphi_2 = \varphi_3 = 0$.

Theorem 4. *If an extremal trajectory contains any doubly-singular point, then every point of the trajectory is doubly-singular.*

Theorem 5. *Every pair of singular points of an extremal trajectory is contained in a single singular interval, or is separated by a generic point.*

Theorem 6. *The number of control switches in an extremal trajectory is finite, and upper-bounded by a constant that depends only on* λ_0.

In section 7, we will show that for *optimal* trajectories, a much stronger property holds: the number of control switches is never greater than 18.

Theorem 7. *Consider a singular interval of non-zero duration, with* $\varphi_i = 0$. *At every point of the interval,* $y = \sin\theta_i = 0$, *and the controls are constant:* $v_i = 0$, *and* $v_j = -v_k = \pm 1$.

Theorem 8. *Consider a doubly-singular interval of non-zero duration, with* $\varphi_i = \varphi_j = 0$. *Along the interval, (i)* $y = \pm 1, \cos\theta_k = 0$, *and (ii) the controls are constant, with* $v_k = \pm 1$, *and* $v_i = v_j = \mp .5$.

5 Extremal controls

Theorems 1, 6, 7, and 8 imply that optimal trajectories are composed of a finite number of segments, along each of which the controls are constant. Considering all possible combinations of signs and zeros of the switching functions allows the twenty extremal controls to be enumerated; table 1 shows the results. The vehicle may spin in place, follow a circular arc, translate in a direction perpendicular to the line joining two wheels, or translate in a direction parallel to the line joining two wheels. We denote each control by a symbol: $\mathrm{P}_{\pm}$, $\mathrm{C}_{i\pm}$, $\mathrm{S}_{i,j}$, or $\mathrm{D}_{k\pm}$, respectively. The subscripts depend on the specific signs of the switching functions.

Theorem 2 gives a more geometric interpretation of the extremal controls. The controls depend on the location of the switching points relative to the switching line. There are four cases:

- **Spin in place.** If the vehicle is far from the switching line, all of the switching points are on the same side of the line, and all of the wheels spin in the same direction. Figure 3(a) shows an example. If the robot is to the left of the switching line, the robot spins clockwise (P_-); if the robot is to the right of the switching line, the robot spins counterclockwise (P_+).
- **Circular arc.** Figure 3(b) shows an example of a counterclockwise arc around IC2 (C_{2+}). If two switching points are on one side of the line, and one switching point is on the other, two wheels spin in one direction at full speed, and one wheel spins in the opposite direction at full speed. These controls cause the vehicle to follow a circular arc of radius four; the center of the arc is the IC corresponding to the switching point that is not on the same side of the switching line as the others, and the direction of rotation depends on whether this switching point is to the left or right of the line.

Symbol	φ	u	λ_0
P_-	+++	-1, -1, -1	$3y$
P_+	---	1, 1, 1	$-3y$
C_{1-}	-++	1, -1, -1	$y + 4\sin\theta_1$
C_{2-}	+-+	-1, 1, -1	$y + 4\sin\theta_2$
C_{3-}	++-	-1, -1, 1	$y + 4\sin\theta_3$
C_{1+}	+--	-1, 1, 1	$-y - 4\sin\theta_1$
C_{2+}	-+-	1, -1, 1	$-y - 4\sin\theta_2$
C_{3+}	--+	1, 1, -1	$-y - 4\sin\theta_3$

Symbol	φ	u	λ_0
$\mathrm{S}_{1,3}$	-0+	1, 0, -1	$2\sqrt{3}$
$\mathrm{S}_{1,2}$	-+0	1, -1, 0	$2\sqrt{3}$
$\mathrm{S}_{3,2}$	0+-	0, -1, 1	$2\sqrt{3}$
$\mathrm{S}_{3,1}$	+0-	-1, 0, 1	$2\sqrt{3}$
$\mathrm{S}_{2,1}$	+-0	-1, 1, 0	$2\sqrt{3}$
$\mathrm{S}_{2,3}$	0-+	0, 1, -1	$2\sqrt{3}$
D_{3+}	00+	.5, .5, -1	3
D_{1-}	-00	1, -.5, -.5	3
D_{2+}	0+0	.5, -1, .5	3
D_{3-}	00-	-.5, -.5, 1	3
D_{1+}	+00	-1, .5, .5	3
D_{2-}	0-0	-.5, 1, -.5	3

Table 1: The twenty extremal controls.

- **Singular translation.** Figure 3(c) shows an example, $\mathrm{S}_{1,3}$, where the second switching point slides along the switching line. If two switching points are an equal distance from the switching line but on opposite sides of the line, two of the wheels spin at full speed, but in opposite direction. If the last switching point falls exactly on the switching line, theorem 2 does not provide any information about the speed of the last wheel. If the wheel does not spin, then the vehicle translates along the switching line, as described by theorem 7. Otherwise, the singular translation is only instantaneous.
- **Doubly-singular translation.** Figure 3(b) shows an example, D_{3+}, where the first and second switching points slide along the switching line. If two switching points fall on the switching line, the speeds of the corresponding wheels cannot be determined from theorem 2. If these wheels spin at half speed, in a direction opposite to that of the third wheel, both switching points slide along the switching line, and the vehicle translates. It turns out that that doubly-singular controls, although extremal, are *never* optimal; see section 7.

6 Classification of extremal trajectories

Every extremal trajectory is generated by a sequence of constant controls from table 1. However, not every sequence is extremal. This section geometrically enumerates the five structures of extremal trajectories.

First consider an example, shown in figure 4(a). Initially, switching points 1 and 3 fall to the left of the switching line, and switching point 2 falls to the right of the switching line. The vehicle rotates in the clockwise direction about IC 2. After some amount of rotation, switching point 2 crosses the switching line. Now all three switching points are to the left of the switching line, the velocity of wheel 2 changes sign, and the vehicle spins in place. When switching point 3 crosses the switching line, the vehicle begins to rotate about IC 3. When switching point 3 crosses back to the left side, the vehicle spins in place again until switching point 1 crosses the

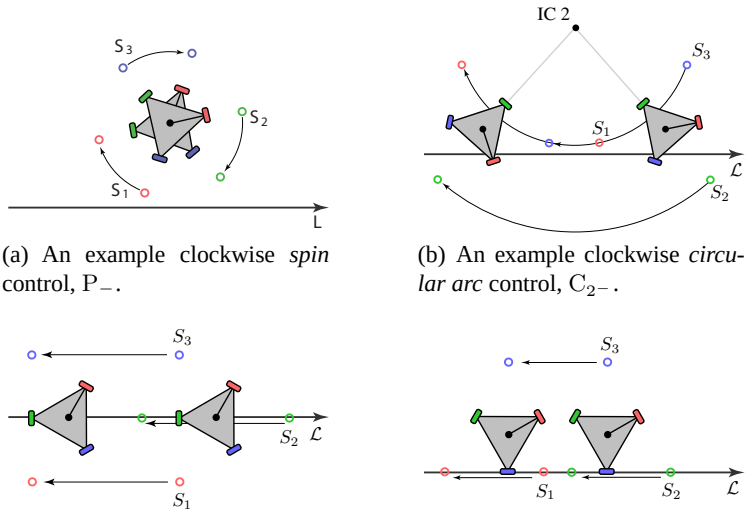

(a) An example clockwise *spin* control, P_-.

(b) An example clockwise *circular arc* control, C_{2-}.

(c) An example *singular translation* control, $\mathrm{S}_{1,3}$.

(d) An example *doubly-singular translation* control, D_{3+}.

Fig. 3: Extremal controls for an omni-directional robot.

line. The pattern continues in this form; we describe the trajectory by the sequence of symbols $\mathrm{C}_{3+}\mathrm{C}_{2-}\mathrm{C}_{1+}\mathrm{P}_+ \ldots$.

In general, if no switching points fall on the switching line (the generic case), then the controls are completely determined by theorem 2, and the vehicle either spins in place or rotates around a fixed point. When one of the switching points crosses the switching line, the controls change. For some configurations for which one or two of the switching points fall exactly on the switching line (the singular and doubly-singular cases), there exist controls that allow the switching points to slide along the switching line.

We will define these classes more rigorously in sections 6.1 and 6.2. However, we can see geometrically that there are five cases:

- **SpinCW** and **SpinCCW**. If the vehicle is far from the switching line, the switching points are on the same side of the switching line and never cross it; the vehicle spins in place indefinitely. The structure off the trajectory is either P_- (if the vehicle is to the left of the switching line) or P_+ (if the vehicle is to the right of the switching line). An example is shown in figure 3(a).
- **RollCW** and **RollCCW**. If the switching points either straddle the switching line, or the vehicle is close enough to the switching line that spinning in place will eventually cause the switching points to straddle the line, the trajectory is a sequence of circular arcs and spins in place. If the vehicle is far enough from the switching line that every switching point crosses the switching line and returns to the same side before the next switching point crosses the line, the structure of the

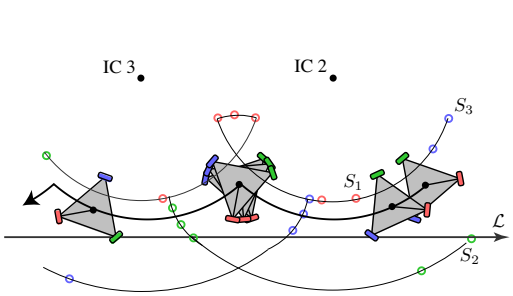

(a) An example trajectory of type **RollCW**, $\mathrm{C}_{2-}\mathrm{P}_{-}\mathrm{C}_{3-}\mathrm{P}_{-}\mathrm{C}_{1-}$.

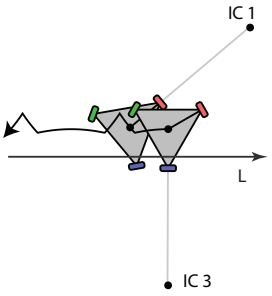

(b) An example trajectory of type **Shuffle**, $\mathrm{C}_{3+}\mathrm{C}_{1-}\mathrm{P}_{-}\mathrm{C}_{2-}\mathrm{C}_{3+}\mathrm{C}_{1-}\mathrm{P}_{-}\ldots$

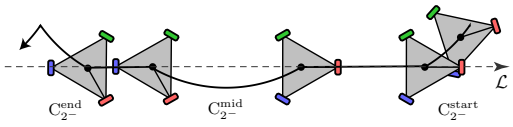

(c) An example trajectory of type **Tangent**, $\mathrm{C}^{\mathrm{start}}_{2-}\mathrm{S}_{2,3}\mathrm{C}^{\mathrm{mid}}_{2-}\mathrm{S}_{2,1}\mathrm{C}^{\mathrm{end}}_{2-}\mathrm{P}_{-}\mathrm{C}^{\mathrm{start}}_{3-}$.

Fig. 4: Extremal trajectories for an omni-directional robot.

trajectory is as described in the example above and in figure 4(a). θ is monotonic during the trajectory.

- **Shuffle**. If the vehicle is close enough to the switching line that two switching points cross the switching line before the first returns to its initial side, the sign of $\dot{\theta}$ changes during the trajectory. An example is shown in figure 4(b).
- **Tangent**. As the vehicle spins in place or follows a circular arc, the switching points follow circular arcs. If one of these arcs is tangent to the switching line, a singular control becomes possible at the point of tangency, and the vehicle may translate along the switching line for an arbitrary duration before returning to following a circular arc. An example is shown in figure 4(c). A single circular arc is divided into three segments in a *tangent* trajectory. These segments are separated by the singular S curves, possibly of zero duration. We call these segments $\mathrm{C}^{\mathrm{start}}$, $\mathrm{C}^{\mathrm{mid}}$, and $\mathrm{C}^{\mathrm{end}}$, as shown in figure 4(c). The robot rotates through $60°$ during a complete $\mathrm{C}^{\mathrm{mid}}$ segment.
- **Slide**. If two switching points fall on the switching line, the trajectory is doubly singular. The vehicle slides along the switching line in a pure translation; an example of this trajectory type is shown by figure 3(d). Although *slide* trajectories are extremal, we will show in section 7 that they are never optimal.

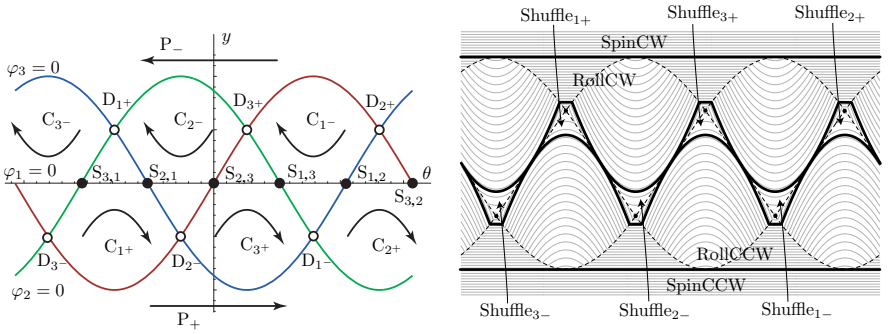

(a) The sinusoidal switching curves partition the configuration space into eight C and P control regions.

(b) Each trajectory corresponds to a level set (contour) of the Hamiltonian. The dashed lines represent control switches; the bold lines separate the trajectory classes.

Fig. 5: The configuration space of the robot relative to the switching line.

6.1 Configuration space

In order to show that the above list of trajectory classes is exhaustive, it is useful to consider the structure of trajectories in configuration space. The configuration of the robot relative to the switching line may be represented by (θ, y). Figure 5(a) shows the configuration space.

Each point on figure 5(a) corresponds to a configuration of the robot relative to the switching line. The sinusoidal curves defined by $\varphi_1 = 0$, $\varphi_2 = 0$, and $\varphi_3 = 0$ mark boundaries in configuration space; we call these curves the *switching curves*. The switching curves and their intersections divide the configuration space into cells, within each of which the controls are constant.

As an example, consider a point below switching curve 1, but above switching curves 2 and 3. The controls are $(-1, 1, 1)$, described by the symbol C_{1-} ; the vehicle follows a circular arc around IC 1 in the clockwise direction. This trajectory is a sinusoidal curve in configuration space.

6.2 Level sets of the Hamiltonian

The trajectory curves in configuration space can be drawn by considering each possible initial configuration, determining the constant control, and integrating to find the trajectory. When the trajectory crosses a switching curve, the control switches. However, the condition that the Hamiltonian remain constant over a trajectory provides an even simpler way to enumerate all trajectories in the configuration space.

Each extremal trajectory falls on a level set of the Hamiltonian (equation 12), and extremal trajectories may be classified by the value λ_0. Figure 5(b) shows the level sets of the Hamiltonian, or equivalently, extremal trajectories in configuration space.

- If $\lambda_0 > 6$, the level set is a pair of horizontal lines, one with $y = \lambda_0/3$, corresponding to a *spinCW* trajectory, and one with $y = -\lambda_0/3$, corresponding to a *spinCCW* trajectory.
- If $2\sqrt{3} \leq \lambda_0 \leq 6$, the level set is composed of two disjoint curves, one corresponding to *rollCW* trajectory and one corresponding to a *rollCCW* trajectory.
- If $\lambda_0 = 2\sqrt{3}$, the level set is the union of the bold curves shown in figure 5(b). Tangent trajectories follow these curves.
- If $3 < \lambda_0 < 2\sqrt{3}$, the level set is composed of six disjoint curves, one corresponding to each of the six symmetric *shuffle* trajectories.
- If $\lambda_0 = 3$, the level set is six isolated points, each corresponding to one of the six *slide* trajectories.

Class	Control sequence	Value of λ_0
SpinCW	P_-	$\lambda_0 \geq 6$
SpinCCW	P_+	
RollCW	$\mathrm{C}_{3-}\mathrm{P}_-\mathrm{C}_{2-}\mathrm{P}_-\mathrm{C}_{1-}\mathrm{P}_- \ldots$	$2\sqrt{3} \leq \lambda_0 < 6$
RollCCW	$\mathrm{C}_{1+}\mathrm{P}_+\mathrm{C}_{2+}\mathrm{P}_+\mathrm{C}_{3+}\mathrm{P}_+ \ldots$	
Tangent	$\mathrm{CSCSCP} \ldots$	$\lambda_0 = 2\sqrt{3}$
$\mathrm{Shuffle}_{1-}$	$\mathrm{C}_{2+}\mathrm{C}_{1-}\mathrm{C}_{3+}\mathrm{P}_+$	$3 < \lambda_0 < 2\sqrt{3}$
$\mathrm{Shuffle}_{2-}$	$\mathrm{C}_{3+}\mathrm{C}_{2-}\mathrm{C}_{1+}\mathrm{P}_+ \ldots$	
$\mathrm{Shuffle}_{3-}$	$\mathrm{C}_{1+}\mathrm{C}_{3-}\mathrm{C}_{2+}\mathrm{P}_+ \ldots$	
$\mathrm{Shuffle}_{1+}$	$\mathrm{C}_{3-}\mathrm{C}_{1+}\mathrm{C}_{2-}\mathrm{P}_- \ldots$	
$\mathrm{Shuffle}_{2+}$	$\mathrm{C}_{1-}\mathrm{C}_{2+}\mathrm{C}_{3-}\mathrm{P}_- \ldots$	
$\mathrm{Shuffle}_{3+}$	$\mathrm{C}_{2-}\mathrm{C}_{3+}\mathrm{C}_{1-}\mathrm{P}_- \ldots$	

Table 2: Four of the five classes of extremal trajectories. Every optimal trajectory is composed of a sequence of controls that is a subsequence of one of the above types. (Doubly-singular *slide* trajectories are extremal, but never optimal; see section 7.) The structure of *tangent* trajectories is complicated, and shown explicitly in figure 6.

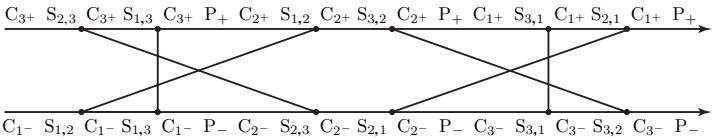

Fig. 6: The structure of *tangent* trajectories. The controls must occur in left-to-right order in the direction shown by either the top or the bottom arrows. However, after a singular control S, the trajectory may switch from one sequence to the other, as shown by the vertical and diagonal lines segments.

7 Optimal trajectories

We have presented the five classes of extremal trajectory; every optimal trajectory must be extremal. However, not all extremal trajectories are optimal. In this section, we will present further conditions that optimal trajectories must satisfy. Specifically, we will show that doubly-singular slide trajectories are never optimal, and that the number of control switches in any optimal trajectory never exceeds 18. Finally, we show that the classification $\{$*spin, roll, shuffle, tangent*$\}$ is *minimal*; for each trajectory class, there exists at least one pair of configurations for which a trajectory of that class is optimal.

Theorem 9. *Doubly-singular slide trajectories are not optimal for any pair of start and goal configurations.*

Proof: (sketch) First show that there exists a *shuffle* that connects any two configurations on a slide that are separated by less than $8\sqrt{6}/3$. Express the distance traveled and the time taken by a *shuffle* trajectory as a function of λ_0. Finally, show that the average forward velocity for such a trajectory is strictly less than -1 (the velocity for the doubly singular trajectory). ■

Theorem 10. *Optimal trajectories contain no more than 18 control switches. Specifically,*

(i) optimal spin trajectories contain zero control switches, and the maximum duration of an optimal spin trajectory is π;
(ii) optimal roll trajectories contain at most 8 control switches;
(iii) optimal shuffle trajectories contain at most 7 control switches;
(iv) optimal tangent trajectories contain at most 12 control switches if the trajectory is non-monotonic in θ, and at most 18 control switches if the trajectory is monotonic in θ;

Proof: (Sketch) The proof for *spin* trajectories is obvious. For each of *roll*, *shuffle*, and *tangent* trajectories we slice, reorder, or reflect segments to construct alternative trajectories that take the same time, but are not extremal. Since these equal-cost trajectories are not extremal, neither these nor the original *roll*, *shuffle*, and *tangent* are optimal. ■

Theorem 11. *There exist bounds on the displacements along the x and θ axis beyond which spin, roll, and shuffle trajectories are not optimal. In particular,*

(i) Roll trajectories with x-displacement more than $\frac{-40\sqrt{2}}{\sqrt{3}}$ are not optimal.
(ii) Shuffle trajectories with x-displacement more than $\frac{-16\sqrt{2}}{\sqrt{3}}$ and θ displacement more than 60° are not optimal.
(iii) Tangent trajectories are not optimal for configurations that are separated by more than 120°, with distance between the configurations less than 4.

Proof: (Sketch) Theorem 10 gives the maximum number of segments that comprise optimal trajectories of each class. We compute the distance of each segment for each class. ■

Theorem 12. *Spin, Roll, Shuffle, and Tangent trajectories are each optimal for at least one pair of start and goal configurations of the omni-directional vehicle.*

Proof: (Sketch) For each class, we explicitly construct a pair of start and goal configurations for which no other trajectory class is optimal. For example, if the goal is sufficiently far away, no *roll*, *spin*, or *shuffle* trajectory can be optimal, since there are no more than nine segments, and each segment is of bounded length. Therefore a *tangent* trajectory is optimal. ■

8 Open problems

We have presented a complete and minimal classification of optimal trajectories, and explicit descriptions of each trajectory. However, we have not addressed the problem of determining which of these trajectories is optimal for a particular pair of start and finish configurations. For the problem of determining the shortest trajectories for a steered car, Reeds and Shepp [9] suggest the simple approach of enumerating all possible structures that connect two configurations, and comparing the time of each. A similar approach should be possible for the omnidirectional vehicle.

Souères and Laumond [13] determined the complete *synthesis* of optimal trajectories for the steered car: an explicit mapping from pairs of configurations to trajectories. Balkcom and Mason [1] determined the synthesis for differential-drive vehicles. Such a result for the omnidirectional vehicle would remove the need for enumerating and comparing all trajectories between a pair of configurations, and would give the metric on the configuration space more explicitly.

The current work also does not consider the presence of obstacles. We expect that optimal trajectories among obstacles would consist of segments of obstacle-free trajectories, and segments that follow the boundary of the obstacles.

There are also broader questions. The shortest or fastest trajectories are now known for a few examples of specific systems: steered cars, the differential drive, and the omni-directional vehicle considered here. The results share some features in common; each of the optimal trajectories can be described by motion of the robot relative to a switching line in the plane. The trajectories for steered cars include arcs of circles and straight lines; the trajectories for differential drives include spins in place and straight lines. The trajectories for the current system include straight lines, arcs of circles, and spins in place, and the system could in that sense be considered a hybrid of a steered car and a differential drive. What generalizations are possible, and can the optimal trajectories be determined for a generic mechanism whose design is described in terms of a set of variable parameters? Which mechanism should be chosen to be most efficient for a given distribution of start and goal configurations?

9 Acknowledgments

The authors would like to thank Steven LaValle, Hamid Chitsaz, Jean-Paul Laumond, Bruce Donald, the members of the CMU Center for the Foundations of Robotics, and the members of the Dartmouth Robotics Lab for invaluable advice and guidance in this work.

References

1. D. J. Balkcom and M. T. Mason. Time optimal trajectories for differential drive vehicles. *International Journal of Robotics Research*, 21(3):199–217, 2002.
2. H. Chitsaz, S. M. LaValle, D. J. Balkcom, and M. T. Mason. Minimum wheel-rotation paths for differential-drive mobile robots. In *IEEE International Conference on Robotics and Automation*, 2006. To appear.
3. M. Chyba and T. Haberkorn. Designing efficient trajectories for underwater vehicles using geometric control theory. In *24rd International Conference on Offshore Mechanics and Artic Engineering*, Halkidiki, Greece, 2005.
4. A. T. Coombs and A. D. Lewis. Optimal control for a simplified hovercraft model. Preprint.
5. G. Desaulniers. On shortest paths for a car-like robot maneuvering around obstacles. *Robotics and Autonomous Systems*, 17:139–148, 1996.
6. L. E. Dubins. On curves of minimal length with a constraint on average curvature and with prescribed initial and terminal positions and tangents. *American Journal of Mathematics*, 79:497–516, 1957.
7. T. Kalmár-Nagy, R. D'Andrea, and P. Ganguly. Near-optimal dynamic trajectory generation and control of an omnidirectional vehicle. *Robotics and Autonomous Systems*, 46:47–64, 2004.
8. L. S. Pontryagin, V. G. Boltyanskii, R. V. Gamkrelidze, and E. F. Mishchenko. *The Mathematical Theory of Optimal Processes*. John Wiley, 1962.
9. J. A. Reeds and L. A. Shepp. Optimal paths for a car that goes both forwards and backwards. *Pacific Journal of Mathematics*, 145(2):367–393, 1990.
10. D. B. Reister and F. G. Pin. Time-optimal trajectories for mobile robots with two independently driven wheels. *International Journal of Robotics Research*, 13(1):38–54, February 1994.
11. M. Renaud and J.-Y. Fourquet. Minimum time motion of a mobile robot with two independent acceleration-driven wheels. In *Proceedings of the 1997 IEEE International Conference on Robotics and Automation*, pages 2608–2613, 1997.
12. P. Souères and J.-D. Boissonnat. Optimal trajectories for nonholonomic mobile robots. In J.-P. Laumond, editor, *Robot Motion Planning and Control*, pages 93–170. Springer, 1998.
13. P. Souères and J.-P. Laumond. Shortest paths synthesis for a car-like robot. *IEEE Transactions on Automatic Control*, 41(5):672–688, May 1996.
14. H. Sussmann and G. Tang. Shortest paths for the Reeds-Shepp car: a worked out example of the use of geometric techniques in nonlinear optimal control. SYCON 91-10, Department of Mathematics, Rutgers University, New Brunswick, NJ 08903, 1991.
15. M. Vendittelli, J. Laumond, and C. Nissoux. Obstacle distance for car-like robots. *IEEE Transactions on Robotics and Automation*, 15(4):678–691, 1999.